# Electron-Spin-Dependent Terahertz Light Transport in Spintronic-Plasmonic Media

K. J. Chau,[1] Mark Johnson,[2] and A. Y. Elezzabi[1]

[1]*Ultrafast Photonics and Nano-Optics Laboratory, Department of Electrical and Computer Engineering, University of Alberta, Edmonton, Alberta, Canada T6G 2V4*

[2]*Naval Research Laboratory, Washington, D.C. 20375-5320, USA*

(Received 8 November 2006; revised manuscript received 31 January 2007; published 29 March 2007)

In this Letter, we demonstrate that electron spin can influence near-field mediated light propagation through a dense ensemble of subwavelength bimetallic ferromagnetic/nonmagnetic microparticles. In particular, we show that ferromagnetic particles coated with nonmagnetic metal nanolayers exhibit an enhanced magnetic field controlled attenuation of the electromagnetic field propagated through the sample. The mechanism is related to dynamic, electromagnetically induced electron spin accumulation in the nonmagnet. The discovery of an electron spin phenomenon in the light interaction with metallic particles opens the door to the marriage of spintronic and plasmonic technologies and could pave the way for the development of light-based devices that exploit the electron spin state.

DOI: 10.1103/PhysRevLett.98.133901 PACS numbers: 42.25.Dd, 72.25.Ba, 72.25.Mk, 73.20.Mf

The study of light interaction with subwavelength composite materials continues to attract basic research attention. Such interest is motivated in part by the potential development of dense, ultrafast optical information technology based on near-field phenomena. Recently, we have shown that ensembles of subwavelength size metallic microparticles exhibit high electromagnetic transparency due to strong near-field dipole-dipole coupling between closely spaced particles [1,2]. Such media exhibit optical properties sensitive to the particles' electrical and magnetic characteristics because electromagnetic propagation through these dense particle collections is mediated by dipolar fields associated with induced surface charges (nonresonant particle plasmons) [1–4]. Here, we demonstrate a new and interesting magnetic phenomenon: a thin film of a nonmagnetic ($N$) material coating ferromagnetic ($F$) particles gives rise to extremely large, magnetic field dependent modulation of the particles' transparency. Collections of uncoated $F$ particles have demonstrated magnetic field dependent attenuation that was shown to result from anisotropic magnetoresistance (AMR) [5]. The magnetic effect for the coated $F$ particles differs because the dependence on the field angle is unique and the magnitude of the attenuation is an order of magnitude larger. We show that the marked enhancement of the magnetic modulation in the coated particles arises from spin-dependent effects in the nonmagnet layer. Spin-polarized charge driven by the incident electromagnetic field across a ferromagnet/nonmagnet ($F/N$) interface over time scales comparable to the spin relaxation time in $N$ behaves as localized spin-polarized currents that generate nonequilibrium spin accumulation in $N$ and create a field dependent interface resistance. Our novel experimental results, presented with a semiquantitative model of nonequilibrium spin accumulation in the $N$ layer, represent a unique manifestation of electron spin effects in the light interaction with metallic microparticles.

To study this spin-dependent photonic phenomenon, we have employed three $F/N$ particle ensembles consisting of Co particles partially coated with several Au layers. Each $45 \pm 2$ nm thick layer is sputter deposited on Co particles ensembles having dimensions ranging from 40 to 140 $\mu$m and an average dimension of $74 \pm 23$ $\mu$m. A single deposition coats the exposed regions of the Co particles. The distributed Au coverage is increased by reorienting the particle collections after each deposition to expose fresh, uncovered Co particles and redepositing another $45 \pm 2$ nm thick Au layer. This procedure is repeated to achieve the desired Au coverage of the particle ensemble. X-ray photoelectron spectroscopy analysis reveals that the percentage Au surface compositions of the three samples are $35 \pm 2\%$, $42 \pm 2\%$, and $77 \pm 2\%$. Our model is introduced in the conceptual illustration in Fig. 1(a). A single-cycle 1 picosecond (ps) pulse that is incident on a bulk collection of subwavelength sized Co/Au particles is transported across a length of order 1 mm because of near-field dipole-dipole coupling. When incident on any individual

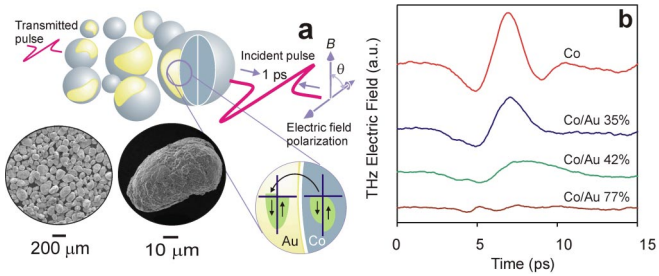


FIG. 1 (color online). (a) Illustration of near-field dipole-dipole coupled transport across a chain of Co/Au bimetallic particles. Spin accumulation at the $F/N$ bimetallic interfaces gives rise to a magnetically modulated interface resistance. (b) Time-domain THz transmission signals through 3 mm thick particle ensembles having varying Au coverage, in zero field.

 

particle, the pulse induces transient spin accumulation in the Au layer resulting in excess resistance at the Co/Au interface.

We access the dynamic, temporal characteristics of the transmitted electric field using broadband terahertz (THz) radiation and time-domain spectroscopy. Single-cycle, linearly polarized, 1 ps wide THz pulses, centered at 0.6 THz with a 1 THz bandwidth, are generated from a GaAs photoconductive switch excited with $<20$ fs, 800 nm laser pulses. The THz pulses are directed towards a 3 mm thick polystyrene sample cell housing the randomly oriented Co/Au particles, and the average transmitted THz electric field, $E_t(t)$, is detected via an optically gated $\langle 111 \rangle$ ZnSe electro-optic crystal. The particles are packed into the sample cell to achieve a filling fraction of $0.50 \pm 0.05$. A plunger lightly depresses on the particle collection in the sample cell to ensure that the fill fraction remains constant during the experimentation period.

The incident electric field pulse $E_i(t)$ induces dipolar surface charges on the bimetallic $F/N$ microparticles [3]. It should be noted that in the THz regime, the real part of the permittivity for Co and Au is on the order of $-10^5$, thus precluding plasmon resonance effects on the particles. The current densities $j(t)$ associated with the nonresonant particle plasmons [1,2,5] exist within the skin depth $\delta \sim 100$ nm from the particle surface. Currents crossing the $F/N$ interface of area $A$ respond to the total resistance within a volume $\sim \delta A$ via Ohm's law $j(t) \alpha E_i(t)/[R_{\mathrm{tot}}(B)A]$, where $R_{\mathrm{tot}}(B)$ is the sum of several contributions:

$$R_{\mathrm{tot}}(B) = R_{\mathrm{Au}} + R_{\mathrm{Co}}(B) + R_i + R_{\mathrm{spin}}(B), \qquad (1)$$

where $R_{\mathrm{Au}}$ is the resistance of Au, $R_{\mathrm{Co}}(B)$ is the resistance of Co incorporating the magnetic field dependent resistance due to AMR, $R_i$ is the intrinsic nonmagnetic interface resistance between the metals, and $R_{\mathrm{spin}}(B)$ is the spin-dependent interface resistance. By means of near-field dipole-dipole coupling, resistivity changes within $\delta$ of the particle surface result in a modulation of the electromagnetic fields propagated through the sample.

We first examine the role of the bimetallic $F/N$ interface on the transmission through the Co/Au particles in zero field. The field $E_t(t)$ transmitted through Co particle samples having 0%, 35%, 42%, and 77% Au surface coverages [Fig. 1(b)] indicates that the Au layer causes drastic reduction of the transmissivity independent of magnetic field or electron spin effects. As Au coverage increases from 0 to 77%, the amplitude is attenuated by $91 \pm 3\%$. The attenuation cannot arise from the inherent resistivity of the Au layer, which is much less than that of Co. The marked attenuation that increases with increasing Au coverage is instead attributed to the introduction of an interface resistance at the Co/Au boundary, $R_i$, which is proportional to the coverage area [6,7].

We next examine the effects of a magnetic field. Analogous to electrically driven current in multilayer $F/N$ systems, the optically driven surface charge on the $F/N$ particles exist in a medium where the resistivity is magnetically influenced via AMR through $R_{\mathrm{Co}}(B)$, spin accumulation effects through $R_{\mathrm{spin}}(B)$, or both. We can discriminate between these contributions by varying the direction of applied field. Figures 2(a) and 2(b) show that the transmission through the Co (0% Au) sample exhibits attenuation and delay due to AMR. In a field $B_\perp$ perpendicular to the electric field polarization [Fig. 2(a)] negligible attenuation and negligible pulse reshaping are observed, whereas both substantial amplitude reduction and pulse reshaping are observed in a parallel field $B_\parallel$ [Fig. 2(b)].

We first consider THz pulse transmission through Co and Co/Au particles in $B_\parallel$ where both AMR and spin accumulation effects may occur. Figures 2(d) and 2(f) show $E_t(t)$ in the presence of a dc magnetic field $B_\parallel = 150$ mT (light traces) in comparison with $E_t(t)$ in the absence of a magnetic field (dark traces). Pulses transmitted through the Co/Au 35% sample, depicted in Fig. 2(d), show increased magnetically induced attenuation, pulse reshaping, and delay relative to the Co (0% Au) sample when $B_\parallel$ is applied. Similar behavior with greater magnetically induced attenuation, pulse reshaping, and delay is seen in the data for the Co/Au 42% sample

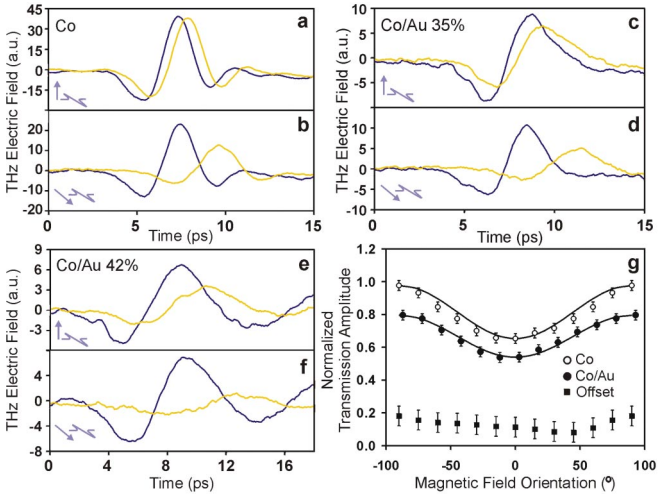


FIG. 2 (color online). Time-domain THz transmission through (a) Co (0% Au) ($B_\perp$), (b) Co (0% Au) ($B_\parallel$), (c) Co/Au 35% ($B_\perp$), (d) Co/Au 35% ($B_\parallel$), (e) Co/Au 42% ($B_\perp$), and (f) Co/Au 42% ($B_\parallel$) particle ensembles for $|B| = 0$ T (dark traces) and $|B| = 150$ mT (light traces). The diagrams depict the orientation of the $B$ field (arrow) relative to the electric field polarization. (g) Normalized transmission amplitude through 3 mm thick Co (open circle) and Co/Au (solid circle) particle samples versus the field angle relative to the incident polarization, where $B = 160$ mT. The transmission amplitudes for both samples have been normalized to their respective zero-field amplitudes, and the data have been fitted with $\cos^2\theta$ functions shown by the solid lines. Solid squares represent the offset between the curves for the Co and Co/Au samples. Within error, the offset is independent of the $B$ orientation.

[Fig. 2(f)]. These $B$-dependent trends of transmission amplitude and delay for $B_{\|}$ are quantified in Figs. 3(a) and 3(b). Referring to Fig. 3(a), for an increase in $B_{\|}$ from 0 to 150 mT, $|E_t(t)|$ decreases by 28 ± 3%, 54 ± 3%, and 73 ± 3% for the Co (0% Au), Co/Au 35%, and Co/Au 42% samples, respectively. The $B$-dependent electric field attenuation in the Co/Au 42% sample is about 3 times greater than that in uncoated Co particles or, equivalently, the intensity attenuation is about an order of magnitude greater. Such marked attenuations are accompanied by large temporal delays (relative to their zero-field transmissions) as shown in Fig. 3(b) and pulse reshaping. Remarkably, magnetically induced attenuation, pulse reshaping, and delay increase with increasing nonmagnetic Au coverage of the Co particles. These effects are caused by enhanced magnetoresistance in the Co/Au particles.

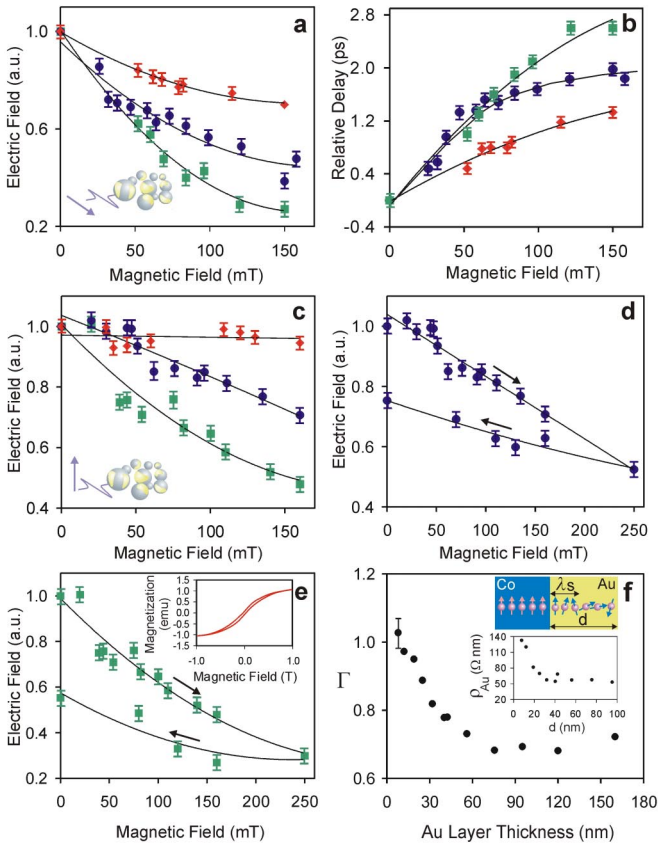


FIG. 3 (color online). (a) Normalized THz electric field amplitude transmitted through Co (0% Au) (diamonds), Co/Au 35% (circles) and Co/Au 42% (squares) particle ensembles versus magnetic field strength in the $B_{\|}$ configuration. The Co/Au 42% samples have about an order of magnitude more intensity attenuation than uncoated Co particles in a magnetic field of $B_{\|}$ = 150 mT. (b) Delay of $E_t(t)$ transmitted through Co (0% Au) (diamonds), Co/Au 35% (circles) and Co/Au 42% (squares) particle ensembles versus magnetic field strength for the $B_{\|}$ configuration. (c) Normalized THz electric field amplitude transmitted through Co (0% Au) (diamonds), Co/Au 35% (circles), and Co/Au 42% (squares) particle ensembles versus magnetic field strength in the $B_{\perp}$ configuration. The normalized transmitted electric field amplitude versus $B_{\perp}$ for the Co/Au 35% and Co/Au 42% particle ensembles are shown in (d) and (e), respectively. The diagrams in the inset of (a) and (c) depict the $B$ orientation (arrow) relative to the electric field polarization. The inset in (e) shows magnetization measurements of the Co particles up to ±1.0 T. (f) Normalized, time-averaged electric field amplitude (in an applied field of $B_{\perp}$ = 160 mT) transmitted through 3 mm thick samples of Co/Au particles versus the Au film thickness, $d$. The upper inset in (f) depicts an illustration of spin accumulation in the Au layer. The lower inset in (f) shows the resistivity measured using a four-point probe technique on witness Au films deposited on glass slides.

Spin accumulation will occur in the $F/N$ microparticles when the surface domains of the Co particles are much larger than the spin diffusion length in the Au film. This requires the magnetization to be uniform in any direction and is therefore isotropic with respect to field angle. To demonstrate this property of the Co/Au samples, we show in Fig. 2(g) the transmission amplitude for 3 mm thick Co and Co/Au samples versus the field angle $\theta$ with respect to the electric field polarization. Both curves have been normalized to their $B = 0$ mT amplitudes, respectively. As seen in Fig. 2(g), the transmission amplitude for the Co ensemble exhibits a $\cos^2\theta$ dependence, providing evidence of AMR. The curve for the Co/Au sample also shows a $\cos^2\theta$ dependence but is offset from the curve for the Co sample by a constant amount that is independent of $\theta$ within experimental error. This offset indicates isotropically enhanced $B$-dependent losses in the Co/Au particles and corresponds to the $\theta$-independent spin contribution to the magnetic attenuation in the coated particles. It is noteworthy that at $\theta = \pm 90°$, the normalized transmission through the Co sample is nearly unity, since AMR is negligible. Thus, spin accumulation effects in the Co/Au samples can be studied with minimal AMR effects by simply reorienting $B$ to 90° with respect to the electric field polarization vector. As shown in Fig. 2(a), the field $E_t(t)$ transmitted through Co (0% Au) particles in $B_{\perp}$ shows insignificant attenuation ($< 2\%$). In comparison, $E_t(t)$ transmitted through the Co/Au 35% and Co/Au 42% samples [Figs. 2(c) and 2(e)] exhibit large magnetically induced attenuation in a $B_{\perp}$ field. This behavior is shown quantitatively in Fig. 3(c). As illustrated in this plot, $|E_t(t)|$ is substantially attenuated by 25 ± 3% and 52 ± 3% for the Co/Au 35% and Co/Au 42% samples, respectively, at a field $B_{\perp}$ = 150 mT. Furthermore, in contrast with the temporal behavior of $E_t(t)$ in a $B_{\|}$ field, $E_t(t)$ in a $B_{\perp}$ field is characterized by a much shorter magnetically induced temporal delay. This is evidence that the origin of the $B$-dependent pulse attenuation, and therefore of the magnetoresistance, in a $B_{\perp}$ field is different from the $B$-dependent effects observed in $B_{\|}$ (which include both spin accumulation and AMR mechanisms).

An essential characteristic of spin-dependent effects in spintronic devices is the hysteretic behavior of the magnetoresistance under magnetic field cycling. As shown in Figs. 3(d) and 3(e), by cycling $B_{\perp}$ from zero to 250 mT

and then back to zero, we observe magnetoresistance hysteresis and remanence in the Co/Au samples. At the return of the $B$ cycle, the zero-field amplitudes of $E_t(t)$ are reduced by $25 \pm 3\%$ and $45 \pm 3\%$ for the Co/Au 35% and Co/Au 42% samples, respectively. The hysteresis and remanence of the THz transmission is consistent with magnetization measurements of the Co particles shown in the inset of Fig. 3(e) that indicate an inflection point in the magnetization at 300 mT, saturation at $\sim$1 T, and hysteresis upon magnetic field cycling.

A fundamental quantitative parameter that governs spin accumulation in Au is the spin diffusion length $\lambda_s$, which determines the spatial extent of nonequilibrium spin injection into the nonmagnet [8]. To support our model and to investigate the relationship between the Au film thickness, $d$, and $\lambda_s$, we perform additional experiments in a field $B_\perp$ with 13 Co/Au samples having identical Au surface coverages but variable Au layer thicknesses ranging from 0 to 160 nm. In discussing our semiquantitative model, the single-cycle THz pulse drives spin-polarized conduction electrons across the $F/N$ interface for a time $\sim$1 ps. Effects that arise from dynamics on a time scale $>$1 ps can have no effect on the attenuation of the transient pulse. The diffusion length for the limiting time of $\tau_i = 1$ ps is $\lambda_i = \sqrt{D\tau_i} = 85$ nm, where $D$ is deduced using an Einstein relation and the resistivity $\rho_{\mathrm{Au}}$ of the Au film (refer to inset of Fig. 3(f) and note that $\rho_{\mathrm{Au}}$ is approximately constant for $d > 40$ nm). In this transient experiment, the interface resistance from spin accumulation is not expected to change for samples with $d > \lambda_i$ because diffusing carriers cannot reach portions of any film thicker than $\lambda_i$. The diffusive spin accumulation model is not valid for $d$ comparable with the electron mean free path, on the order of tens of nm. The resistivity, mean scattering time, and spin relaxation time are all very sensitive to film morphology, and data in this range of $d$ do not merit a rigorous fit. However, a valid prediction of the model is that the interface resistance will be determined by spin accumulation within a spin depth $\lambda_s = \sqrt{D\tau_s}$, where $\tau_s$ is the spin relaxation time in the Au film, for any sample with $d > \lambda_s$ [9]. The spin-dependent interface resistance is [10]

$$R_{\mathrm{spin}}(d > \lambda_s) = P^2 \rho_{\mathrm{Au}} \lambda_s / A, \qquad (2)$$

where $P$ is the fractional polarization of electrons crossing the interface.

As shown in Fig. 3(f), the normalized, time-averaged, field dependent transmission, $\Gamma = \langle E_t(160\ \mathrm{mT})\rangle / \langle E_t(0\ \mathrm{mT})\rangle$, is very sensitive to small values of $d$ but changes little for $d > 75$ nm. These data are consistent with our prediction that $R_{\mathrm{spin}}$ should not change for $d > \lambda_i$. The asymptotic approach to a constant value also permits us to identify a lower bound for the spin diffusion length, $\lambda_s = 75$ nm.

Using this value of $\lambda_s$, a measured value $\rho_{\mathrm{Au}} = 5.5 \times 10^{-8}\ \Omega\,\mathrm{m}$, and a typical value of $P$ in the range 20% to 40%, we obtain an estimate of the interface resistance contribution arising from spin accumulation from Eq. (2) to be in the range $R_{\mathrm{spin}}A = 2 \times 10^{-16}\ \Omega\,\mathrm{m}^2$ to $7 \times 10^{-16}\ \Omega\,\mathrm{m}^2$. As discussed above, the nonmagnetic, spin-independent attenuation effects that we report are believed to be entirely dominated by interface resistance. The calculated contribution to interface resistance from spin accumulation ranges between 8% and 29% of the field independent contribution from interface resistance, $R_iA = 2.4 \times 10^{-15}\ \Omega\,\mathrm{m}^2$ [6]. There is reasonable agreement, given the limitations of our semiquantitative model, between the calculation and the 30% attenuation observed in Fig. 3(f) for $d > 75$ nm.

A lower bound for the spin relaxation time $T_2$ that corresponds with $\lambda_s = 75$ nm is $T_2 = \tau_s = \lambda_s^2/D \approx 1$ ps. Using a Drude scattering time of $\tau = 12$ fs (derived from $\rho_{\mathrm{Au}} = 5.5 \times 10^{-8}\ \Omega\,\mathrm{m}$), a spin flip probability of $a = \tau/T_2 = 1 \times 10^{-2}$ is obtained, as an upper bound. This is in good agreement with a previously measured value for Ag films of $a = 4.0 \pm 0.5 \times 10^{-3}$ [6].

Now that a new spin-dependent plasmon transport phenomenon has been shown, a novel avenue has been opened in both the fields of spintronics and photonics. The ability to magnetically manipulate near-field mediated light transport through metallic particles via electron spin promises another degree of freedom in the development of light-based information devices.

This work was supported by the Natural Sciences and Engineering Research Council of Canada (NSERC). M. J. gratefully acknowledges the support of the Office of Naval Research (ONR), through contract No. N0001405AF00002.

[1] K. J. Chau, G. D. Dice, and A. Y. Elezzabi, Phys. Rev. Lett. **94**, 173904 (2005).
[2] K. J. Chau and A. Y. Elezzabi, Phys. Rev. B **72**, 075110 (2005).
[3] H. C. van de Hulst, *Light Scattering by Small Particles* (Dover Publications, New York, 1957).
[4] A. J. L. Adam, J. Brok, A. S. van de Nes, and P. C. M. Planken, in *Conference Digest of the 2006 Joint 31st International Conference on Infrared and Millimeter Waves and 14th International Conference on Terahertz Electronics, Shanghai, China* (IEEE, Piscataway, NJ, 2006), p. 15.
[5] K. J. Chau and A. Y. Elezzabi, Phys. Rev. Lett. **96**, 033903 (2006).
[6] R. Godfrey and Mark Johnson, Phys. Rev. Lett. **96**, 136601 (2006). Note that these contact resistance measurements were made using Permalloy–Ag layers.
[7] K. J. Chau and A. Y. Elezzabi, Phys. Rev. B **73**, 085419 (2006).
[8] I. Žutić, J. Fabian, and S. Das Sarma, Rev. Mod. Phys. **76**, 323 (2004).
[9] Mark Johnson and R. H. Silsbee, Phys. Rev. B **35**, 4959 (1987), refer to the appendix.
[10] Mark Johnson, J. Appl. Phys. **75**, 6714 (1994).